Complex structural contribution of the morphotropic phase boundary in Na0.5Bi0.5TiO3 - CaTiO3 system

Roy Roukos, Sara Abou Dargham, Jimmy Romanos, Fatima Barakat, Denis Chaumont

Complex Structural Contribution of the Morphotropic Phase Boundary in $Na_{0.5}Bi_{0.5}TiO_3$ - $CaTiO_3$ system

Roy Roukos [a,*], Sara Abou Dargham [b], Jimmy Romanos [b], Fatima Barakat [b] and Denis Chaumont [a]

[a] *Laboratoire Interdisciplinaire Carnot de Bourgogne UMR 6303 CNRS-Université de Bourgogne 9 Avenue Alain Savary, BP 47870, F-21078 Dijon Cedex, France*

[b] *Department of Natural Science, Lebanese American University (LAU), Byblos, Lebanon*

Abstract

The correlation between structure and dielectric properties of lead-free (1-x)$Na_{0.5}Bi_{0.5}TiO_3$ - x$CaTiO_3$ ((1-x)NBT - xCT) polycrystalline ceramics was investigated systematically by X-ray diffraction, combined with impedance spectroscopy for dielectric characterizations. The system shows high miscibility in the entire composition range. A morphotropic phase boundary (MPB), at $0.09 \leq x < 0.15$ was identified where rhombohedral and orthorhombic symmetries coexist at room temperature. The fraction of orthorhombic phase increases gradually with x in the MPB region. Dielectric measurements reveal that the relative permittivity increase with addition of Ca^{2+}. This behavior is unusual with this kind of doping. A thermal hysteresis occurred only in the MPB composition which varies in a non-monotonically manner with x, detected by dielectric properties. This phenomenon is related to the crystalline microstructure by a linear relationship between the fraction of each phase and dielectric properties, and, more precisely, to the strong interaction between rhombohedral and orthorhombic phases.

Keywords: Morphotropic Phase Boundary, X-Ray Diffraction, Dielectric Properties, Thermal Hysteresis, NBT-CT

1. Introduction

Lead oxide ferroelectric ceramics (such as PZT) are widely used in various electronic devices such as transducers, actuators, MEMS, capacitors and Random Access Memory (RAM) [1]. However, due to the toxic effect of lead, the development of alternative lead-free ferroelectric materials able to replace PZT in microelectronics is currently pursued worldwide.

Among the different varieties of lead-free materials, $Na_{0.5}Bi_{0.5}TiO_3$(NBT) is considered one of most promising ferroelectric materials showing equivalent properties as PZT[2]. Although NBT system presents a complex behavior, it has shown interesting features: (i) good ferroelectric properties at room temperature with strong remanent polarization *(Pr ~ 38 μC.cm-2)* [3-5], (ii) high Curie temperature(T_C ~ 320 ˚C) [6], (iii) special sequence of phase transition as a function of temperature [7-9] and finally, (iv) it can form solid solutions with other perovskites which appears in phase diagrams as a biphasic domain called *Morphotropic Phase Boundary (MPB)*. Around this region, NBT and $BaTiO_3$ (BT) solid solution systems exhibit improved properties [10]. In addition to NBT-BT, other families of NBT-based solid solutions have been developed in order to understand the MPB behavior of this material. Among these solutions, the (1-x)NBT – xCT system shows excellent piezoelectric and ferroelectric properties at the rhombohedral – tetragonal MPB [11, 12]. Despite the succession of structural changes obtained in this region, the exact behavior of the MPB remains unclear.

First of all, it is crucial to differentiate between a normal biphasic domain and a Morphotropic Phase Boundary (MPB). A “MPB” is a biphasic zone constituted by a mixture of two phases with different crystal structures, with variable composition but always identical. In other words, the two phases of same compositions exist (NBT-BT rhombohedral + NBT-KBT tetragonal at x = 0.07[13] for example) at room temperature; the fraction of each phase and the lattice parameters change with x (% of doping).While, in a “normal biphasic domain”, the compositions of the two phases are different ($x_1 \neq x_2$), and their proportion varies with x, but

always have the same characteristics as that x_1 and x_2 and finally, the lattice parameters remain constant with x.

Several systems were studied in order to determine the compositional range of MPB [14, 15] and to establish the physical and structural properties. However, there are inconsistencies in its location. In NBT – BT, the MPB was found around x = 6-7 %[16], where the maximum values of the piezoelectric and dielectric constants were obtained. Rout et al. [18] observed the MPB at x ≈ 5.5 %. Chen et al. [13] revealed the MPB between x = 6-10%, whereas Sung et al. [19] obtained this region around x = 5-7 %. In the other hand, Ge et al. [20] reported that the MPB was located between 5 and 8 %. Recently, Eerd et al. [21]found the MPB of NBT-BT at x = 5.5%. In other system such as NBT – ST ($SrTiO_3$), a specific concentration is never determined; this leads eventually to different values of MPB [15, 22-24]. However, some studies have not obtained the MPB, regardless of the percentage of substitution [25]. Recently, few studies have been carried out on (1-x)NBT – xCT ($CaTiO_3$) system and the MPB region was found at x = 10 % [26].

While many studies were carried out in order to improve the piezoelectric properties of these materials near the MPB compositions; studies concerning the MPB physical behavior were rarely investigated. As it is well known the solid solutions with compositions close to MPB exhibit interesting physical properties. According to Glazer, rhombohedral (R3c) and orthorhombic (Pnma) phases are not related to group-subgroup relationship[27], however a strong relationship between these two phases in the MPB region was suggested. This paper proves that the orthorhombic phase *(Pnma)* contributes to the rhombohedral phase*(R3c)* as shown in dielectric response. This new result gives a proper understanding of the correlation between structure and dielectric properties of lead-free (1-x)$Na_{0.5}Bi_{0.5}TiO_3$ – x$CaTiO_3$ ((1-x)NBT – xCT)) polycrystalline ceramics. Thus, several compositions of (1-x)NBT –xCT ($0 \leq x \leq 1.00$) were prepared focusing on a specific range of Ca^{2+} concentration near the MPB region ($0.07 \leq x \leq$

0.15).The crystalline structure of the prepared ceramics was examined using X-ray diffraction at room temperature. A mixture of two phases *(R3c + Pnma)* is stabilized for ($0.09 \leq x < 0.15$), indicating that rhombohedral phase of NBT is able to undergoes an orthorhombic distortion when increasing Ca^{2+} substitution. The dielectric and aging properties were measured as a function of temperature and frequency. Then, dielectric aspects and structural analysis obtained at room temperature were compared and discussed. These results enable a methodical comparison between the structural models at the MPB such as phase fraction, identified phases and the related dielectric properties

2. Material and methods

$(1-x)N_{0.5}B_{0.5}TiO_3 - xCaTiO_3$powders and ceramics were prepared by a conventional solid state synthesis route. A stoichiometric amount of reagent grade powders of Na_2CO_3, $CaCO_3$, Bi_2O_3, and TiO_2 (purity greater than 99.6%) were mixed and milled in water with Zirconia balls for 2 hours and then dried at 90°C. The mixture was homogenized in a dry mortar and calcined at 750°C for 4 hours. A second calcination at 950°C for 4 hours was required to complete the reaction. After this procedure, the calcined powders were pressed into pellets and sintered in the temperature range 1075 - 1350°C for 1 hour in a confined environment using alumina crucibles. This operation is necessary in order to prevent the exceed volatilization of Bi and Na. The sintering temperature was selected based on Ca^{2+} concentration in each composition.

Bulk densities of all the ceramics were measured by the Archimedes method. Despite the difficulty encountered during sintering; the average values are in a range between 96 – 99%. Sintered samples were polished in order to remove the thin layer of powders adhered to the surface of pellets.

Powders and ceramics X-ray diffraction measurements were performed at room temperature, using a D8 advance X-ray diffractometer (Vantec detector) with $CuK\alpha_1\alpha_2$radiations in the 2θ range of 20° - 90°with a scanning step 0.017° and 2 s/step. Structural analysis and Rietveld refinement were carried out with the Topas (Brucker-AXS) software. For dielectric and aging properties, surfaces of the sintered pellets

were coated with gold electrodes by PVD (physical vapor deposition) procedure. The permittivity (real part, imaginary part and loss tangents) and aging measurements were performed under multi-frequency (100 Hz – 1 MHz) with a precision LCR meter (4284A) in the temperature range of 77 – 450 K.

3. Results and Discussion

X-ray diffraction was used to highlight the change in crystal structure of (1-x)NBT-xCT samples as a function of CT concentration ($0 \leq x \leq 1.00$).Fig. 1.a shows XRD patterns of all (1-x)NBT – xCT systems at room temperature. All samples exhibit a pure ABO_3perovskite structure without any secondary or impurity phases. This implies that Ca^{2+} has diffused into the rhombohedral NBT lattice in order to form a solid solution with a perovskite structure. For all synthesized solid solutions, the XRD patterns obtained are either identical to pure NBT or to pure CT. The increase in Ca content shifts XRD peaks patterns towards higher angle (2θ),, indicating a decrease in cell volume. Fig. 1.b shows XRD patterns taken around the 2θ range 66.8-72°. As known, pure NBT has a rhombohedral phase (*R3c* space group), while CT possesses orthorhombic structure (*Pnma* space group). The rhombohedral symmetry was characterized by $(208)_R$ and $(220)_R$ peaks splitting. Similarly to pure NBT (x = 0), the samples below x = 0.07 exhibit a rhombohedral structure. With increasing x, the symmetry gradually changes from rhombohedral to orthorhombic. From x = 0.09, an additional peak appears, it corresponds to the $(004)_O$ reflection (solid arrow) of the orthorhombic phase. The intensity of this reflection increases with x while the intensity of the rhombohedral peaks gradually decreases until disappearing completely for x = 0.15. The simultaneous presence of the (R+O) peaks in this composition range ($0.09 \leq x < 0.15$) indicate that both orthorhombic and rhombohedral phases coexist. For $x \geq 0.15$, pure orthorhombic phase was obtained, where the XRD patterns are all identical to those of *Pnma* of the pure CT (x = 1.00) phase. This was highlighted by the splitting of the double rhombohedral peak $(208)_R$, $(220)_R$ to quadruplet peak $(400)_O$, $(242)_O$,$(004)_O$ and $(410)_O$ features of the orthorhombic phase. The inset in Fig. 1.a shows the variation of the integrated intensity ratio of $(230)_O$ and $(024)_R$ peaks as a function of x. The evolution of intensity

ratio ($I(230)_O/I(024)_R$) reveals two irregular discontinuities at x = 0.09 and x = 0.15.The sharp break in the intensity ratio $I(230)_O/I(024)_R$ below can be interpreted as a detection of phase transition from rhombohedral to the orthorhombic phase.

It is important to study the behavior of this mixture of two phases *(R3c + Pnma)* in order to know if it is a normal biphasic domain or Morphotropic Phase Boundary (MPB). For this reason, a Rietveld refinement was carried out with a two phase rhombohedral and orthorhombic model to check the variation of the phase fraction of two phases as well as the cell volume for each composition in this region ($0.09 \leq x < 0.15$). R-factors, showing the quality of the fit, are provided in the supplementary material. The evolution of phase fraction (%) at room temperature as a function of x is plotted in Fig. 2.a. While, the fraction of orthorhombic phase increases from 16% to 100% when x increased from x = 0.09 to 0.15, the fraction of rhombohedral phase decreases gradually (from 84% to 38%) in the composition range $0.09 \leq x \leq 0.13$, and disappears completely (0%) at $x \geq 0.15$. This evolution shows that in terms of phases proportions, a normal behavior of a heterogeneous mixture of two solid solutions in biphasic domain is observed. However, the variation in cell volume in this region ($0.07 \leq x < 0.15$) at room temperature (Fig. 2.b) shows an "unusual" behavior of the two phases *(R3c + Pnma)* in the biphasic domain. It's known that in a biphasic domain between two monophasic domains, the cell volume of each of the two phases is constant while the fraction of the two phases change with x. However, in our case, the cell volume of the *R3c* and *Pnma* phases changes continuously with x. In the particular biphasic domain presented in the (1-x)NBT – xCT system ($0.09 \leq x < 0.15$), it was shown that the solid is formed by a mixture of two phases *(R3c + Pnma)*where (i) the two phases present always equal compositions and (ii) the fraction of these two phases will vary with x. In view of this, a strong interaction could occur between these two phases based on their distribution. Based on the properties mentioned in the introduction, this result confirm that the particular biphasic

domain obtained in the (1-x)NBT – xCT between $0.09 \leq x < 0.15$, is a Morphotropic Phase Boundary (MPB).

Fig. 3 shows the temperature dependence of the real part (ε') and the dielectric loss (tanδ) of the relative permittivity for the (1-x)NBT – xCT with x = 0.01,0.05, 0.11, 0.15 0.25, 0.35 and 0.85 at 1 kHz and 10 kHz. All the ceramics exhibit at least one dielectric anomaly. Phase transitions are observed clearly and the peaks become broader with increasing CT concentration. The relative permittivity for x = 0.01 and 0.05 exhibit frequency dispersion and appear as a shoulder which become broad taking the form of a curve at x = 0.11. Moreover, the dispersion is more noticeable on the dielectric loss tanδ(T). The dielectric behavior totally changed for $x \geq 0.15$, the permittivity exhibits strong frequency dependence at the maximum temperature (T_m) suggesting a diffuse phase transition. In this case, the temperature associated to each maximum of the dielectric constant shifts gradually to lower values with increasing x. It is important to note that the tanδ decreases and becomes relatively low with increasing x. The variation of tanδ with frequency also shows a similar behavior as the dielectric permittivity except the maximum broadness of peak.

NBT – xCT with x = 0.01 and 0.05 present the same anomaly that occurred in pure NBT [10, 15, 28] in the ferroelectric state with the stabilization of the rhombohedral structure *(R3c)* at room temperature. In fact, the XRD analysis shows that the system between $0.09 \leq x < 0.15$ is not monophasic; in addition to *R3c* phase, a supplementary $(230)_O$ peak proves the simultaneous presence of the orthorhombic phase *(Pnma)*. The latter is non-polar (centrosymmetric) and hence is not anticipated to show any dielectric anomaly in the temperature range studied. Therefore, the dielectric anomalies obtained in this region are attributed to rhombohedral *(R3c)* phase.

Similar to pure NBT, for x = 0.01 and 0.05 compositions, the first anomaly appears around 440 K know as depolarization temperature (T_d) which is attributed to the transition from ferroelectric state to antiferroelectric state [29]. This transition is accompanied by a structural

change resulting in the instability of the rhombohedral phase *(R3c)* which transits gradually to tetragonal phase *(P4bm)*. Contrary to x = 0.07, the dielectric constant peak of x = 0.15 was depressed and broadened. The maximum of the dielectric anomaly moves toward lower temperature with increasing x, and exhibits a large maximum around the room temperature (T_m = 295 K). This is a characteristic of relaxor behavior, where the fitting by modified Curie-Weiss law $(1/\varepsilon') - (1/\varepsilon_m) = (T - T_m)^{\gamma}/C$ gave a value of $\gamma = 1.53$ (degree of diffuseness). This value shows clearly that this ceramic is ferroelectric relaxor. This behavior may be related to the cations disorder at the A-site complex [30].

For a large temperature range and in the MPB compositions, the permittivity exhibits a *"thermal hysteresis"* depending on x and situated in the temperature range between: 260 – 450 K (x = 0.09), 230 – 430 K (x = 0.10), 210 – 410 K (x = 0.11) and 180 – 360 K (x = 0.13) at 10 kHz. Fig. 4 shows the thermal hysteresis of the (1-x)NBT – xCT in the MPB compositions during heating and cooling at 10 kHz. There is a remarkable characteristic that this cycle exhibits a non-monotonous evolution that didn't exist for $x \leq 0.07$ and appears for x = 0.09. It gradually increases with increasing x up to a maximum and then decreases to disappear for x = 0.15.

Since NBT-CT composition is a heterogeneous mixture of two phases, relaxor ferroelectric phase (F/R-NBT) and paraelectric phase (P-CT). The total permittivity of biphasic domain decreases as x increases. Nevertheless, the permittivity increases with increasing CT (x) if $T \leq$ 220 K. In the MPB compositions (x = 0.09, 0.10, 0.11 and 0.13), the value of ε' is very high compared with x = 0.07 and 0.15 for T > 300 K. As a result, increasing x,ε' drastically increases from ~ 900 (x = 0.07) to ~ 1200 (x = 0.09), reaches a maximum of 1300 for x = 0.10 where the system is biphasic and then gradually decreases to 800 at x = 0.15 where the system becomes monophasic. These original observations can be related to the interaction between the two phases rhombohedral *(R3c: F/R)* and orthorhombic *(Pnma: P)* that leads to a nonlinear behavior as a function of x.

Fig. 5 shows the difference Δε'(T) between the values of the permittivity obtained during heating and those revealed during cooling, as a function of temperature at 10 kHz. From the "full width at half maximum (FWHM)" of Δε'(T) curves, the degree of existence of the hysteresis and the maximum temperature of the hysteresis (T_{mTH}) were determined. Fig. 5 confirms the particular evolution of thermal hysteresis in the MPB compositions. Each curve of Δε' exhibits a maximum. The position of the maximum and their amplitude are highly dependent on x (%Ca). Therefore, there is a strong relationship between the evolution of the thermal hysteresis presented in these materials and its composition x (%Ca); in particular, the strong interaction between the two phases in the MPB compositions is confirmed.

The width evolution of the thermal hysteresis for a given composition, as a function of temperature, is characterized by a peak through a maximum which the corresponding temperature is noted T_{mTH}. It represents the temperature at which the sample has a maximum thermal hysteresis magnitude. The T_{mTH} and the FWHM of Δε'(T) values are represented in the table 1. It is noted that, the T_{mTH} temperature strongly decreases with increasing x; and; even for a low degree of substitution (i.e. from 0.09 to 0.10, ΔT_{mTH}= 27 K). At the same time, the FWHM of Δε'(T) peak increases in with x.

In many ceramics, especially perovskites, the origin of such phenomenon is explained by the formation and detection of a modulated phase [31, 32]. The modulated phase is proposed to explain the thermal hysteresis behavior of pure NBT. In this study, (1-x)NBT – xCT system consists of a mixture of two phases: rhombohedral *(R: R3c)* and orthorhombic *(O: Pnma)*. The behavior of pure NBT is complex especially, in the MPB compositions and in the temperature range between 200°C – 320°C. It seems that the rhombohedral and tetragonal phases can coexist in the thermal hysteresis; which may be responsible for the appearance of this phenomenon [33]. Therefore, the resulting dielectric peak is a response to the electrical and mechanical interactions

between polar and non-polar regions [34]. However, this remains a hypothesis and no experimental procedure was verified.

Therefore, two possible explanations for the observations obtained in this study were considered:

- Assuming that this would be based on the micro-domains model of relaxor ferroelectric, which is the cause of the thermal hysteresis phenomenon [35]. In this case, (1-x)NBT – xCT system with $x \geq 0.15$ should be affected by this phenomenon. Hence, all ceramics appear to behave as relaxor. The same thing could be said for $x \leq 0.07$ where the addition of Ca^{2+}leads to the appearance of polar micro-domains[36]. However, in both cases, no thermal hysteresis is generated.
- A structural origin can also be invoked to explain the existence and evolution of thermal hysteresis as a function of x. In fact, the comparison between the evolution of the magnitude or the intensity of the cycle (normalized) to the percentage (fraction) evolution of the minority phase existing in the MPB compositions (Fig. 6) at room temperature (300 K), shows that there is a strong correlation between the magnitude of the thermal hysteresis and the variation in the proportion of the two phases in the material.

Fig. 6 showed that the amplitude of $\Delta\varepsilon'/\varepsilon'$ cycle increases with x (%Ca^{2+}) where the orthorhombic phase (O) is minority ($x \leq 0.11$). While for $x \geq 0.13$, the amplitude of the cycle $\Delta\varepsilon'/\varepsilon'$ decreases with x and the minority phase become rhombohedral (O: majority). Then, this difference disappears when the system recovers its monophasic state. Another interesting feature is that the $\Delta\varepsilon'/\varepsilon'$ reaches a maximum for an intermediate composition, where the two phases have an equivalent proportion ($x = 0.11$).

Such correlation between the coexistence of two phases and the presence of a dielectric hysteresis cycle in pure NBT was mentioned in literature [32, 37]; previous studies proposed this hypothesis to explain their experimental results but did not have the opportunity to provide the experimental proof. The results obtained in this study bring this confirmation. The correlation between the phase fractions and the width of the cycle is verified. Therefore, the strong interaction between the phases in the biphasic domain (between *F/R (R3c)* phase and *P (Pnma)* phase) with maximum interaction when the two phases are in equivalent proportions has been well demonstrated.

Mechanical and electrical interactions between various existing phases depend on the relative proportions (fraction) of the two phases; this leads to a wide change of the dielectric response which appears as a thermal hysteresis cycle. In this system, the coexistence of two phases (R+O) induces interactions between rhombohedral polar domains and orthorhombic non-polar matrix. At both extremities of MPB compositions, the system is monophasic; for x = 0.15, it is effectively non-polar single phase material (O:*Pnma*), with no thermal hysteresis. On the other hand, for x = 0.07, the system is also monophasic, with rhombohedral polar phase (R: *R3c*), but without thermal hysteresis too. The interaction between polar and non-polar domains is much stronger that the proportions (fraction) of two phases are equal; the maximum is obtained for x = 0.11. Hence, it seems that the main cause of this phenomenon is the coexistence of two phases in this material. Therefore, it appears that the origin of thermal hysteresis is related to the crystal microstructure and, more specifically, the percentage of each phase existing in the MPB compositions.

In order to better understand the complex behavior of the MPB compositions materials, the evolution of the dielectric permittivity as a function of time, called aging was studied. It was carried out at different temperatures and for many ceramics in the MPB compositions. Fig. 7.a shows the evolution of the dielectric permittivity (normalized over the permittivity at t = 0 s) as a

function of time at 10 kHz for x = 0.10 ceramic, where different isothermal conditions were imposed inside the thermal hysteresis at T = 350 K, 380 K and 428 K (Fig. 7.b). It is noted that the permittivity for x = 0.10 system evolves significantly as a function of time. Hence, this system undergoes an aging despite the imposed temperature with a maximum aging obtained at T = 380 K corresponding to the sharp decrease of the dielectric constant. It is important to note that at T = 350 K, the system slightly evolves to reach a maximum at T= 380 K, then the aging decreases again as the temperature increases to T = 428 K. Fig. 7 shows that the aging reaches a maximum concomitant with the maximum of thermal hysteresis reported in Fig. 5.

In order to study the aging for all compositions of the MPB, thermal hysteresis evolution was performed at 10 kHz with the application of an isotherm at T = 350 K (Fig. 8.a). Fig. 8.b shows the evolution of the permittivity (normalized over the permittivity at t = 0 s) as a function of time for different compositions (x = 0.10; 0.11 and 0.13). The aging phenomenon exists despite the value of x its kinetics depending on x; the system exhibits a quick evolution for x = 0.10. This variation considerably increases for x = 0.11 where the system shows high aging kinetics. This kinetic abruptly decreases for x = 0.13 where the system undergoes slight changes at this temperature: the dielectric constant almost decreases. Note that, for x = 0.13, the majority phase is orthorhombic (62% *Pnma*, 38% *R3c*) and hence, this phase is centrosymmetric and does not show any dielectric anomaly. Therefore, there is no phase transition in the temperature range used in this study. This explains the slight variation of the permittivity as a function of time. However, the highest behavior in the aging curves (Fig. 8.a) corresponds to the maximum of the thermal hysteresis phenomenon for x = 0.11 where the two phases *(R3c + Pnma)* have equivalent proportions. In view of this, the aging of these materials is probably due to the change in the relative proportions of the phases between rhombohedral *(R3c)* and orthorhombic *(Pnma)* structures; since the system is biphasic and provides a morphotropic phase boundary (MPB).

4. Conclusion

The combined structural and dielectric properties of Ca^{2+} modified NBT [(1-x)$Na_{0.5}Bi_{0.5}TiO_3$ – x$CaTiO_3$] revealed that the system undergoes a phase transition as a function of the substitution x (%Ca) at room temperature. In addition, the results showed the MPB compositions as a function of x (%Ca) and its relation to dielectric properties. A Morphotropic Phase Boundary (MPB) was detected by XRD analysis between $0.09 \leq x < 0.15$ where the rhombohedral *(R3c)* and orthorhombic *(Pnma)* phases coexist. Thermal hysteresis only occurred in the MPB compositions where its magnitude changes non-monotonically with x. This phenomenon has been attributed to the interaction between the orthorhombic *(Pnma)* and rhombohedral *(R3c)* phases. Maximum thermal hysteresis took place when the two phases had almost equal proportions (x = 0.11). Aging as a function of time, which was revealed by a continuous decrease in the permittivity, showed a maximum when the two phases present equal proportions (x = 0.11). This corresponds to the gradual transformation of the rhombohedral phase to the orthorhombic phase.

Acknowledgements

R. R. thanks the French Ministry of Higher Education and Research for supporting this work. This work was supported by the Nanosciences Department, ICB Laboratory, Université de Bourgogne.

References

[1] G.H. Haertling, Ferroelectric Ceramics: History and Technology, Journal of the American Ceramic Society, 82 (1999) 797-818.
[2] L.B. Kong, J. Ma, W. Zhu, O.K. Tan, Reaction sintering of partially reacted system for PZT ceramics via a high-energy ball milling, Scripta Materialia, 44 (2001) 345-350.
[3] Y. Li, W. Chen, Q. Xu, J. Zhou, X. Gu, Piezoelectric and ferroelectric properties of $Na_{0.5}Bi_{0.5}TiO_3$-$K_{0.5}Bi_{0.5}TiO_3$-$BaTiO_3$ piezoelectric ceramics, Materials Letters, 59 (2005) 1361-1364.
[4] Q. Xu, S. Chen, W. Chen, S. Wu, J. Zhou, H. Sun, Y. Li, Synthesis and piezoelectric and ferroelectric properties of $(Na_{0.5}Bi_{0.5})_{1-x}Ba_xTiO_3$ ceramics, Materials Chemistry and Physics, 90 (2005) 111-115.
[5] Y. Yuan, C.J. Zhao, X.H. Zhou, B. Tang, S.R. Zhang, High-temperature stable dielectrics in Mn-modified (1-x) $Bi_{0.5}Na_{0.5}TiO_3$-x$CaTiO_3$ ceramics, Journal of Electroceramics, 25 (2010) 212-217.
[6] H. Yu, Z.-G. Ye, Dielectric, ferroelectric, and piezoelectric properties of the lead-free $(1-x)(Na_{0.5}Bi_{0.5})TiO_3$-x$BiAlO_3$ solid solution, Applied Physics Letters, 93 (2008) 112902.

[7] G.O. Jones, P.A. Thomas, The tetragonal phase of $Na_{0.5}Bi_{0.5}TiO_3$ - a new variant of the perovskite structure, Acta Crystallographica Section B, 56 (2000) 426-430.
[8] G.O. Jones, P.A. Thomas, Investigation of the structure and phase transitions in the novel A-site substituted distorted perovskite compound $Na_{0.5}Bi_{0.5}TiO_3$, Acta Crystallographica Section B, 58 (2002) 168-178.
[9] L. Luo, W. Ge, J. Li, D. Viehland, C. Farley, R. Bodnar, Q. Zhang, H. Luo, Raman spectroscopic study of $Na_{1/2}Bi_{1/2}TiO_3$-x%$BaTiO_3$ single crystals as a function of temperature and composition, Journal of Applied Physics, 109 (2011) 113507-113506.
[10] C. Xu, D. Lin, K.W. Kwok, Structure, electrical properties and depolarization temperature of $(Bi_{0.5}Na_{0.5})TiO_3$-$BaTiO_3$ lead-free piezoelectric ceramics, Solid State Sciences, 10 (2008) 934-940.
[11] Y. Watanabe, Y. Hiruma, H. Nagata, T. Takenaka, Phase transition temperatures and electrical properties of divalent ions (Ca^{2+}, Sr^{2+} and Ba^{2+}) substituted $(Bi_{1/2}Na_{1/2})TiO_3$ ceramics, Ceramics International, 34 (2008) 761-764.
[12] W. Jo, J.E. Daniels, J.L. Jones, X. Tan, P.A. Thomas, D. Damjanovic, J. Rodel, Evolving morphotropic phase boundary in lead-free $(Bi_{1/2}Na_{1/2})TiO_3$-$BaTiO_3$ piezoceramics, Journal of Applied Physics, 109 (2011) 014110-014117.
[13] M. Chen, Q. Xu, B.H. Kim, B.K. Ahn, J.H. Ko, W.J. Kang, O.J. Nam, Structure and electrical properties of $(Na_{0.5}Bi_{0.5})_{1-x}Ba_xTiO_3$ piezoelectric ceramics, Journal of the European Ceramic Society, 28 (2008) 843-849.
[14] M. Otonicar, S.D. Å kapin, M. Spreitzer, D. Suvorov, Compositional range and electrical properties of the morphotropic phase boundary in the $Na_{0.5}Bi_{0.5}TiO_3$-$K_{0.5}Bi_{0.5}TiO_3$ system, Journal of the European Ceramic Society, 30 (2010) 971-979.
[15] D. Rout, K.-S. Moon, S.-J.L. Kang, I.W. Kim, Dielectric and Raman scattering studies of phase transitions in the (100 - x)$Na_{0.5}Bi_{0.5}TiO_3$--x$SrTiO_3$ system, Journal of Applied Physics, 108 (2010) 084102-084107.
[16] T. Tadashi, M. Kei-ichi, S. Koichiro, $(Bi_{1/2}Na_{1/2})TiO_3$ - $BaTiO_3$ System for Lead-Free Piezoelectric Ceramics, Japanese Journal of Applied Physics, 30 (1991) 2236.
[17] B.-J. Chu, D.-R. Chen, G.-R. Li, Q.-R. Yin, Electrical properties of $Na_{1/2}Bi_{1/2}TiO_3$–$BaTiO_3$ ceramics, Journal of the European Ceramic Society, 22 (2002) 2115-2121.
[18] D. Rout, K.-S. Moon, V.S. Rao, S.-J.L. Kang, Study of the morphotropic phase boundary in the lead-free $Na_{1/2}Bi_{1/2}TiO_3$-$BaTiO_3$ system by Raman spectroscopy, Journal of the Ceramic Society of Japan, 117 (2009) 797-800.
[19] Y.S. Sung, J.M. Kim, J.H. Cho, T.K. Song, M.H. Kim, T.G. Park, notRoles of lattice distortion in (1-x)$(Bi_{0.5}Na_{0.5})TiO_3$ - x$BaTiO_3$ ceramics, Applied Physics Letters, 96 (2010) 202901-202901-202903.
[20] W. Ge, J. Yao, C. DeVreugd, J. Li, D. Viehland, Q. Zhang, H. Luo, Electric field dependent phase stability and structurally bridging orthorhombic phase in $Na_{0.5}Bi_{0.5}TiO_3$ - x%$BaTiO_3$ crystals near the MPB, Solid State Communications, 151 (2011) 71-74.
[21] B. Wylie-van Eerd, D. Damjanovic, N. Klein, N. Setter, J. Trodahl, Structural complexity of $(Na_{0.5}Bi_{0.5})TiO_3$-$BaTiO_3$ as revealed by Raman spectroscopy, Physical Review B, 82 (2010) 104112.
[22] J.-R. Gomah-Pettry, SaÄ±, amp, x, S. d, P. Marchet, J.-P. Mercurio, Sodium-bismuth titanate based lead-free ferroelectric materials, Journal of the European Ceramic Society, 24 (2004) 1165-1169.
[23] J.R. Gomah-Pettry, A.N. Salak, P. Marchet, V.M. Ferreira, J.P. Mercurio, Ferroelectric relaxor behaviour of $Na_{0.5}Bi_{0.5}TiO_3$–$SrTiO_3$ ceramics, physica status solidi (b), 241 (2004) 1949-1956.
[24] Y. Hiruma, Y. Imai, Y. Watanabe, H. Nagata, T. Takenaka, Large electrostrain near the phase transition temperature of $(Bi_{0.5}Na_{0.5})TiO_3$--$SrTiO_3$ ferroelectric ceramics, Applied Physics Letters, 92 (2008) 262904-262903.

[25] W. Krauss, D. SchÃ¼tz, F.A. Mautner, A. Feteira, K. Reichmann, Piezoelectric properties and phase transition temperatures of the solid solution of (1 - x)($Bi_{0.5}Na_{0.5}$)TiO_3-x$SrTiO_3$, Journal of the European Ceramic Society, 30 (2010) 1827-1832.
[26] R. Rajeev, G. Rohini, V. Kothai, A. Anupriya, S. Anatoliy, B. Hans, Phases in the (1 − x)$Na_{0.5}Bi_{0.5}TiO_3$ – (x)$CaTiO_3$ system, Journal of Physics: Condensed Matter, 22 (2010) 075901.
[27] A.M. Glazer, The classification of tilted octahedra in perovskites, Acta Crystallographica Section B, 28 (1972) 3384-3392.
[28] B.-J. Chu, D.-R. Chen, G.-R. Li, Q.-R. Yin, Electrical properties of $Na_{1/2}Bi_{1/2}TiO_3$-$BaTiO_3$ ceramics, Journal of the European Ceramic Society, 22 (2002) 2115-2121.
[29] W. Ting, D. Huiling, S. Xiang, Dielectric and ferroelectric properties of (1-x)$Na_{0.5}Bi_{0.5}TiO_3$-x$SrTiO_3$ lead-free piezoceramics system, Journal of Physics: Conference Series, 152 (2009) 012065.
[30] Y. Li, W. Chen, J. Zhou, Q. Xu, H. Sun, M. Liao, Dielectric and ferroelectric properties of lead-free $Na_{0.5}Bi_{0.5}TiO_3$-$K_{0.5}Bi_{0.5}TiO_3$ ferroelectric ceramics, Ceramics International, 31 (2005) 139-142.
[31] J.M. Kiat, G. Calvarin, J. Schneck, Coexistence of the 1q and 2q incommensurate phases and memory effect in barium sodium niobate, Physical Review B, 49 (1994) 776-785.
[32] M.-L. Zhao, C.-L. Wang, W.-L. Zhong, J.-F. Wang, Z.-F. Li, Grain-Size Effect on the Dielectric Properties of $Bi_{0.5}Na_{0.5}TiO_3$, Chinese Physics Letters, 20 (2003) 290.
[33] J. Suchanicz, J. Kwapulinski, X-ray diffraction study of the phase transitions in $Na_{0.5}Bi_{0.5}TiO_3$, Ferroelectrics, 165 (1995) 249-253.
[34] I.G. Siny, C.S. Tu, V.H. Schmidt, Critical acoustic behavior of the relaxor ferroelectric $Na_{1/2}Bi_{1/2}TiO_3$ in the intertransition region, Physical Review B, 51 (1995) 5659-5665.
[35] J. Fousek, L.E. Cross, Domain-related problems of ferroelectric ceramics, Ceramics International, 30 (2004) 1169-1173.
[36] Y. Yuan, E.Z. Li, B. Li, B. Tang, X.H. Zhou, Effects of Ca and Mn Additions on the Microstructure and Dielectric Properties of ($Bi_{0.5}Na_{0.5}$)TiO_3 Ceramics, Journal of Electronic Materials, 40 (2011) 2234-2239.
[37] G.A. Smolenskii, I. V.A., A. A.I., K. N.N., *New ferroelectrics of complex composition* Soviet Physics - Solid State, 2 (1961) 2651-2654.

List of figures

Fig. 7 (a) thermal hysteresis of x = 0.10 ceramics at 10 kHz, where the dotted lines represent the isotherm imposed on the either side of the maximum of thermal hysteresis. (b) Evolution of the permittivity (ε' normalized over ε'(t = 0)) at 10 kHz as a function of time (s) for 3 isotherms: T = 350, 380 and 428 K imposed within the thermal hysteresis for x = 0.10. The solid line represents the refinement obtained from the equation ofcapacitor discharge: $y = A + B.\exp(-(\frac{t-t0}{\tau})^{\gamma})$.

Fig. 8.a Evolution of the thermal hysteresis for different compositions in the MPB, where the dotted line at T = 350 K represents an isothermal imposed at fixed temperature, in order to studythe aging for all compositions of the MPB. (b) Variation of the permittivity (ε' normalized over ε'(t = 0)) at 10 kHz of (1-x)NBT – xCT for x = 0.10, 0.11 and 0.13 as a function of time (s).

List of Tables

Table1. T_{mTH} and FWHM values of Δε'(T) at MPB composition (x = 0.09, 0.10, 0.11 and 0.13) at 10 kHz.

List of figures

Figure 1

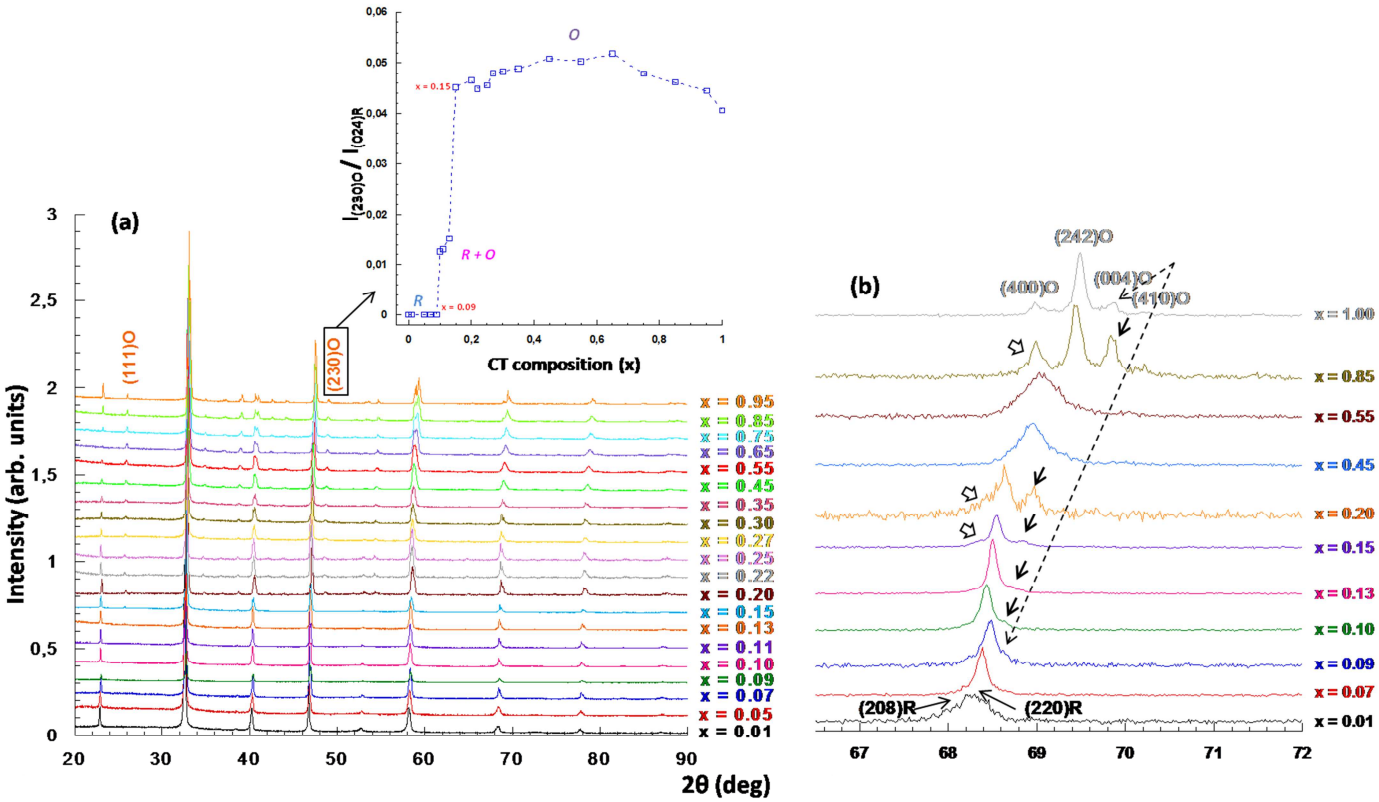

Figure 2

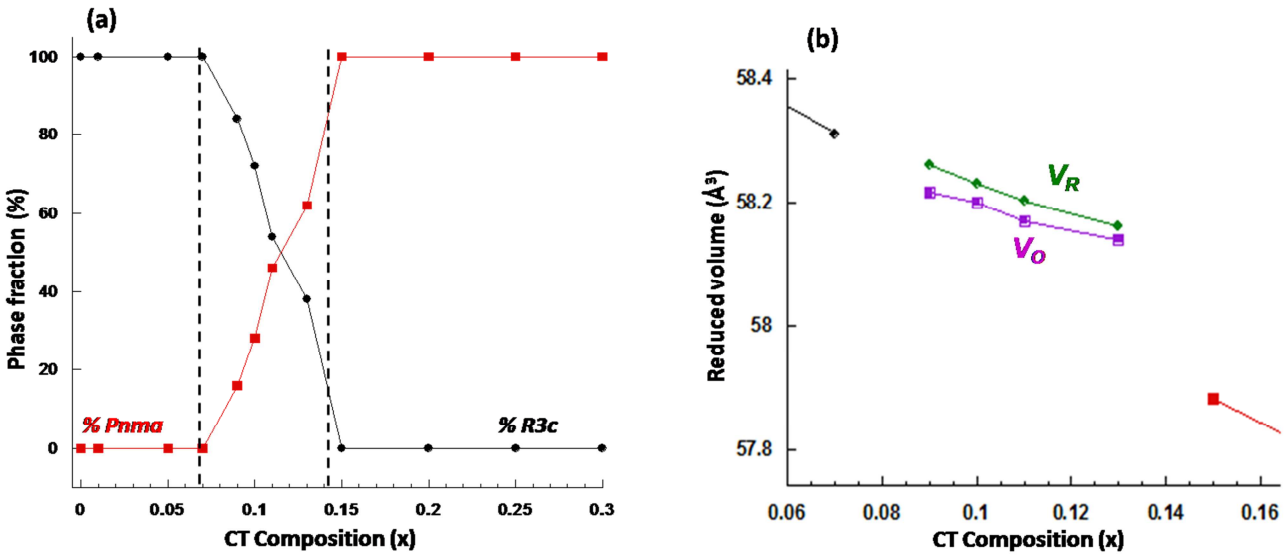

Figure 3

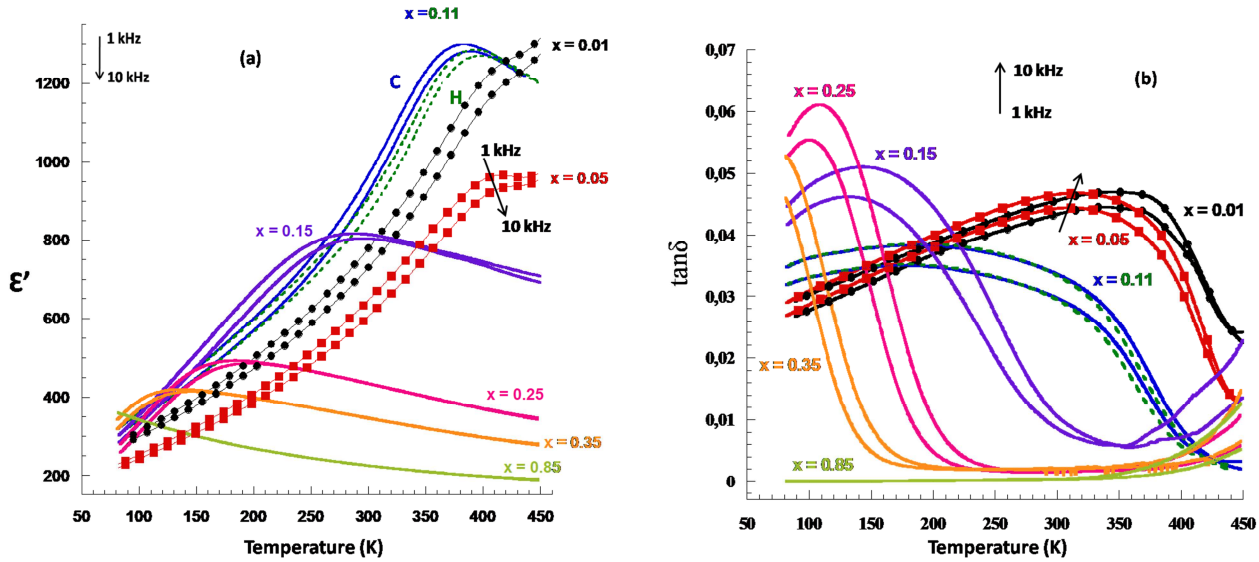

Figure 4

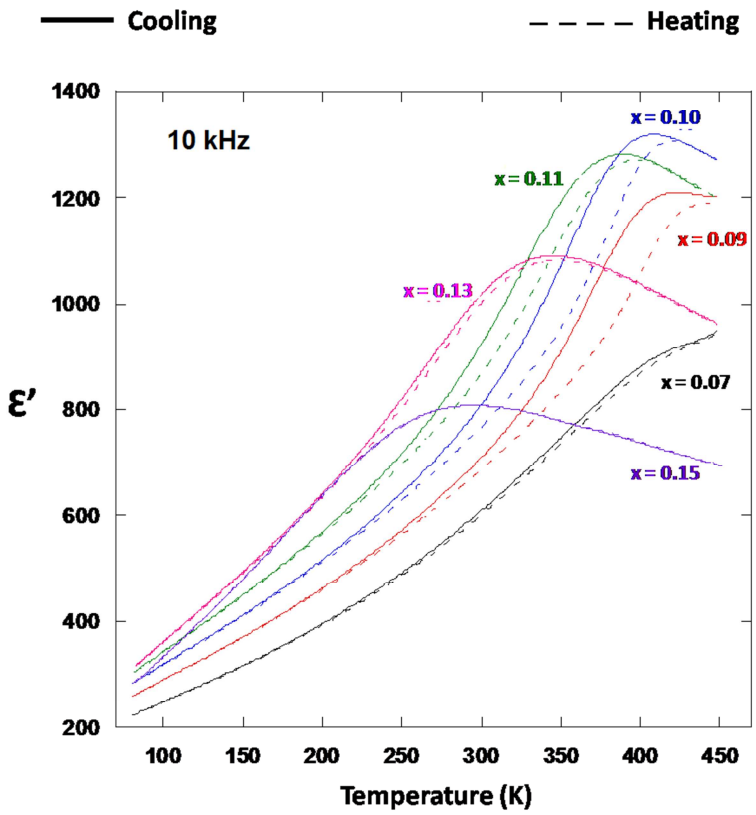

Figure 5

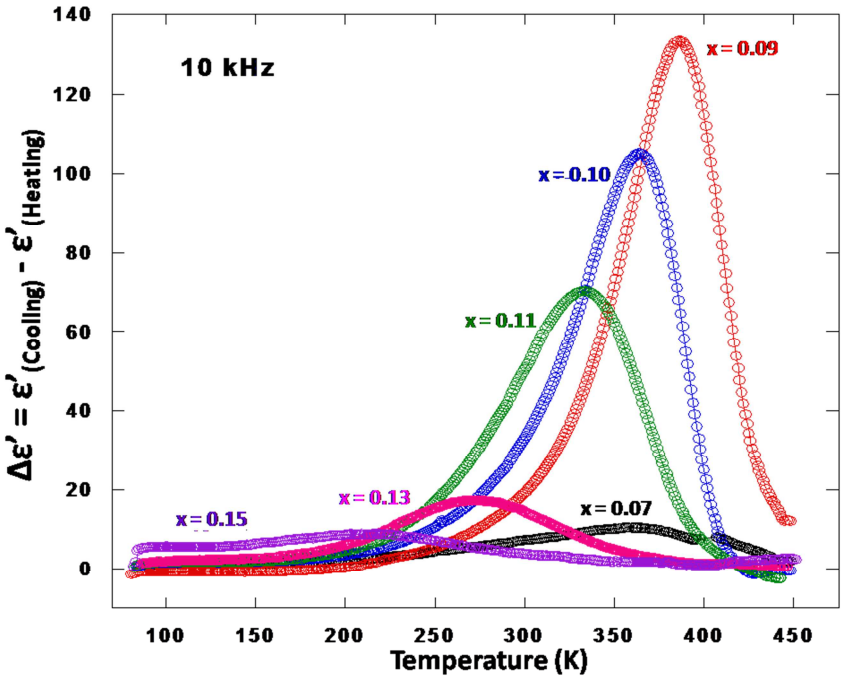
10 kHz
x = 0.09
x = 0.10
x = 0.11
x = 0.13
x = 0.15
x = 0.07
Δε' = ε'(Cooling) - ε'(Heating)
Temperature (K)
140
120
100
80
60
40
20
0
100
150
200
250
300
350
400
450

Figure 6

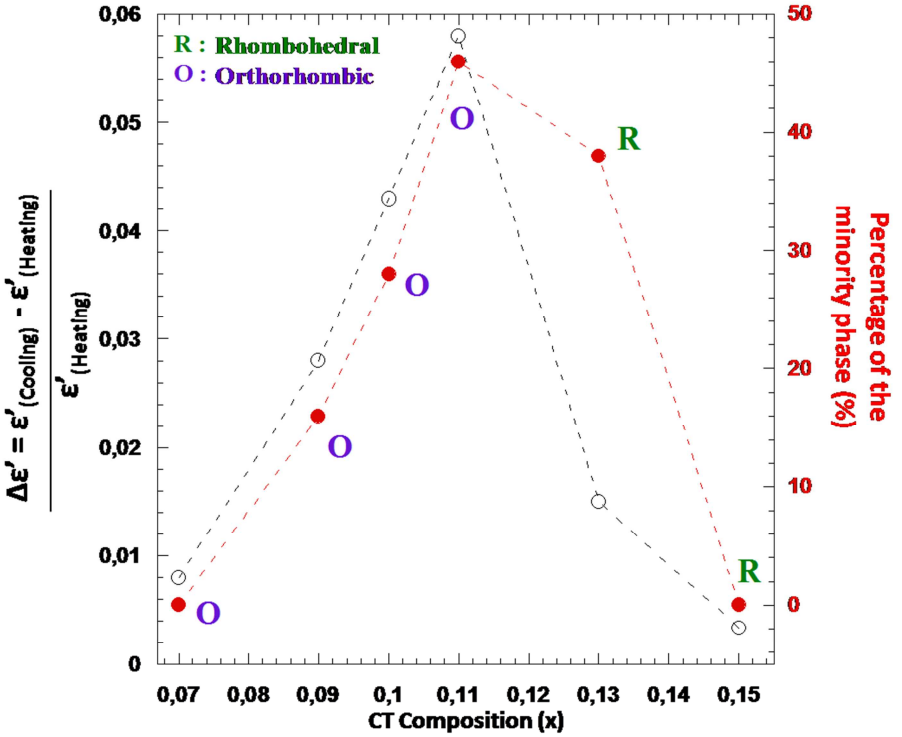
R : Rhombohedral
O : Orthorhombic
Δε' = ε'(Cooling) - ε'(Heating) / ε'(Heating)
Percentage of the minority phase (%)
CT Composition (x)
O
O
O
O
R
R
0,06
0,05
0,04
0,03
0,02
0,01
0
50
40
30
20
10
0
0,07
0,08
0,09
0,1
0,11
0,12
0,13
0,14
0,15

Figure 7

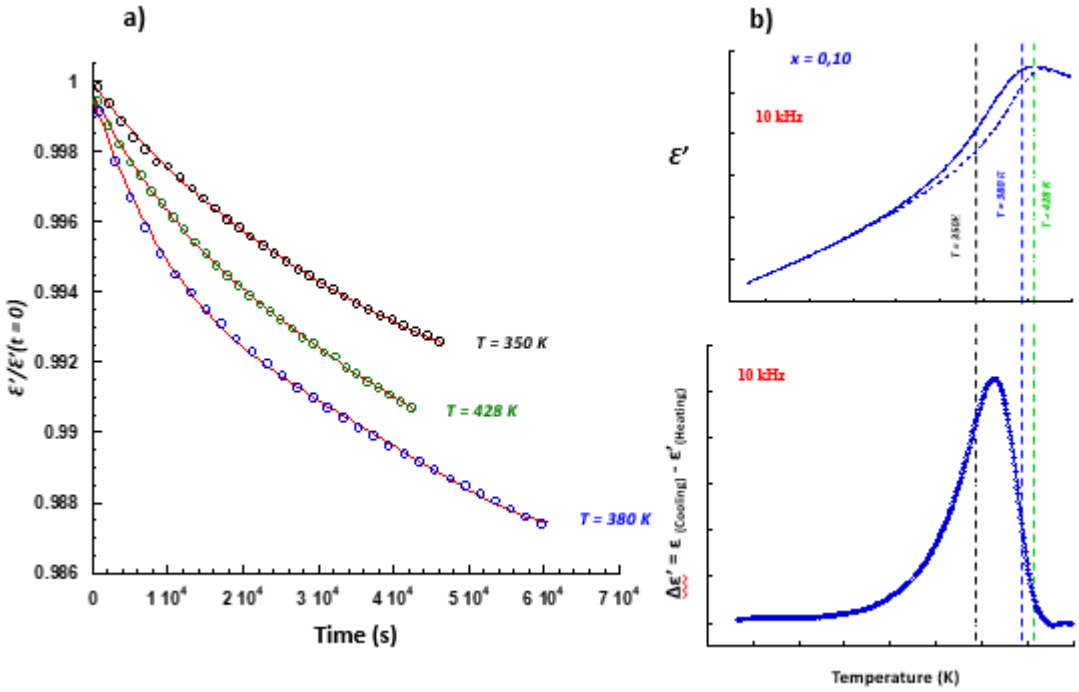

Figure 8

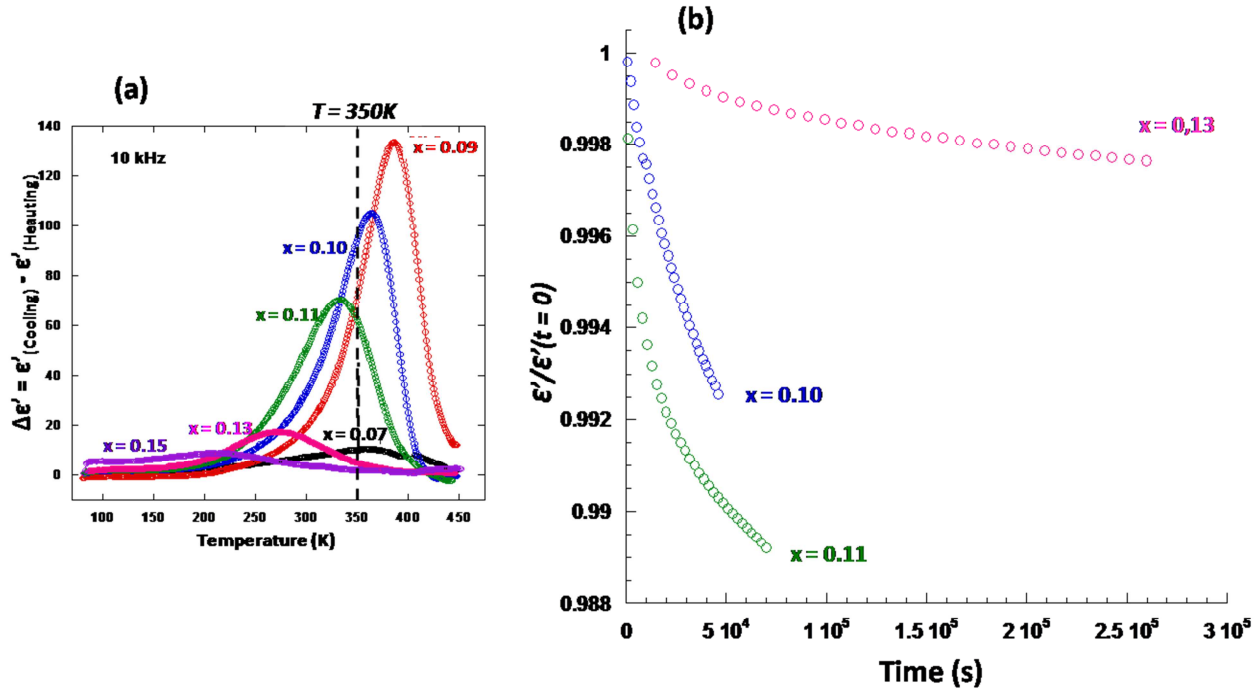

List of tables

Table 1

	MPB composition	
x	T_{mTH} *(K)*	*FWHM (+/-1 K)*
0.09	390	60
0.10	363	71
0.11	332	91
0.13	271	104